MICROSTRUCTURE AND HARDNESS VARIATION IN A TIG WELDMENT OF IRRADIATED F82H —

H. Tanigawa (Japan Atomic Energy Research Institute), N. Hashimoto (Oak Ridge National Laboratory), M. Ando, T. Sawai, K. Shiba (JAERI), R.L. Klueh (ORNL)

OBJECTIVE

The objective of this work is to identify the part of a weld joint that exhibited lower hardening on a HFIR11J irradiated (5dpa 573K) weld joint tensile specimen and investigate the mechanisms occurring by analyzing the corresponding microstructure.

SUMMARY

Previous work reported that a TIG weld joint of F82H exhibited low irradiation hardening in a tensile test, compared to the base metal. Microhardness tests and microstructure observation on the neutron-irradiated TIG weld joint of F82H revealed that the over-tempered zone in the heat-affected zone (HAZ) exhibited this good performance. The region in the HAZ where the prior austenite grain became very fine during welding also exhibited lower irradiation hardening. Hypotheses for these low-hardening mechanisms were proposed based on the phase diagram and grain orientation.

PROGRESS AND STATUS

Introduction

To validate the potential of reduced-activation ferritic/martensitic steel (RAF) as a structural material for fusion power plants, the methodology for joining the steel to form welds with adequate toughness before and after irradiation must be developed. In this study, an irradiated tungsten inert-gas (TIG) weldment (weld metal, base metal and HAZ) of the IEA-modified F82H (F82H-IEA) was investigated. Previous post-irradiation tensile test results of F82H-IEA TIG weldment specimens suggested that the weld metal exhibited almost the same amount of irradiation hardening as the base metal, but the HAZ showed far less hardening than the base metal (Fig. 1) [1]. In this study, a hardness profile across the irradiated weld joint was determined to investigate the location of the weldment that was involved with this low hardening. The mechanisms responsible for this low hardening were investigated in order to provide guidelines for the improvement of radiation resistance of F82H by heat treatment.

Experimental

The materials used for this research were normalized-and-tempered F82H-IEA steel, nominally Fe-7.5Cr-2W-0.15V-0.02Ta-0.1C, in wt%, and an F82H TIG weldment. The TIG welding was performed using pulsed direct current with filler wire for 5 to 6 passes on pre-heated and U-shape grooved 15mm thick plate. The TIG weldment was annealed at 993K for 1 hour. SS-3 type tensile specimens were machined with the HAZ in the middle of the gage section. The details of the welding conditions and specimens were explained in a previous paper [1]. Irradiation was performed in the Oak Ridge National Laboratory (ORNL) High Flux

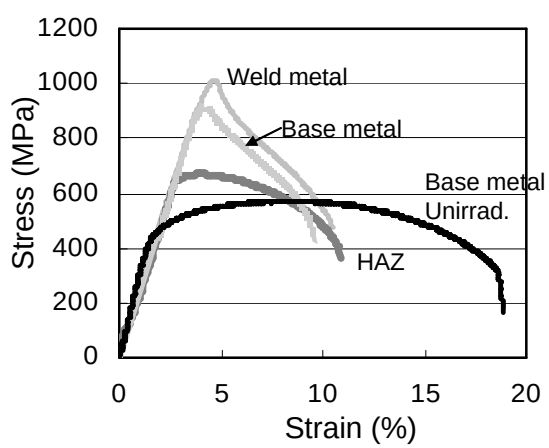

Fig. 1 Tensile results of irradiated weldments and unirradiated base metal [1].

Isotope Reactor (HFIR) up to 5 dpa at 573K. Vickers hardness tests (500 gf load) were carried out along the gage section of the tensile specimens at 254μm (0.010 in) intervals from the weld metal region to the base metal region in order to obtain the micro hardness profile. Five as-prepared specimens and four irradiated specimens were tested, and in total 8 hardness profiles were obtained for each conditions. Specimens were etched with 88% H_2O/10% HNO_3/2% HF prior to the hardness tests in order to perform metallography after the hardness tests to determine hardness-microstructure correlation. Post-irradiation tensile tests were carried out at room temperature at a strain rate of $1x10^{-3}$ s^{-1} on the hardness-tested specimens to identify in which microstructural region the tensile fracture occurred.

Surface observations were performed by Scanning Electron Microscopy (SEM) using FE-SEM (Philips XL30) for unirradiated specimens and conventional SEM (TOPCON ABT-32) for irradiated specimens. For unirradiated specimens, the Orientation Image Mapping (OIM) system (Tex SEM Laboratories) and X-ray energy-dispersive spectrometry (XEDS) system were used to analyze the grain orientation distribution and precipitate distribution, respectively. The OIM analysis was performed with a resolution of 200 nm and a 0.05 s exposure time per spot. The XEDS mapping was done with a resolution of 200 nm and a 4.0 s dwell time per spot.

Results and discussion

The microstructure of the TIG weldment is shown in Fig. 2. The microstructure consisted of 3 regions; i.e., weld metal, HAZ, and base metal. The HAZ can be further divided into 3 regions with obviously different microstructures, and those regions are denoted with a circled number in Fig. 2. Here we call the boundary line between region 1 and region 2 the transformation line, since the α–γ transformation occurred during welding within the region inside these lines. It should be noted that the microstructure of the weld metal was rather fine except for the last pass region, and the HAZ was wider than that of a single-pass weldment, since a multi-pass TIG weld was used in this study.

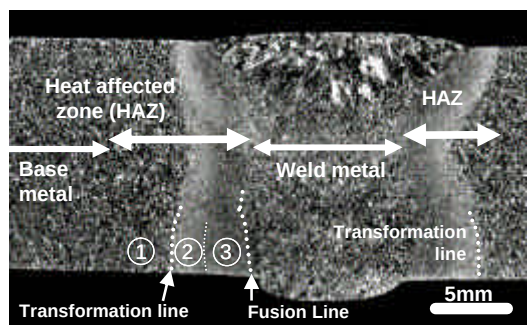

Fig. 2 Micrstructure of TIG weldment and the definitions of the different regions.

The HAZ microstructure of a singe-pass weld on a martensitic steel can be defined as follow [2] (see Fig. 3):

HAZ1 (T_T<T<Ac_1) — The original tempered martensite was heated above the tempering temperature (T_T=1023K), i.e. it was over-tempered. The microstructure is quite similar to that of the base metal as the region was never heated over Ac_1 (the temperature at which austenite begins to form on heating ≅1113K).

HAZ2 (Ac_1<T< Ac_3) — Over-tempered martensite and freshly formed martensite constitute the very fine microstructure, as this region was heated between Ac_1 and Ac_3 (the temperature at which the austenite transformation is complete ≅1193K). The prior austenite grains are generally very fine and ambiguous.

HAZ3 (Ac_3<T<$T_{\gamma\delta}$) — The microstructure is freshly formed martensite. The grains are finer than that of base metal, but larger than in HAZ2. The fine

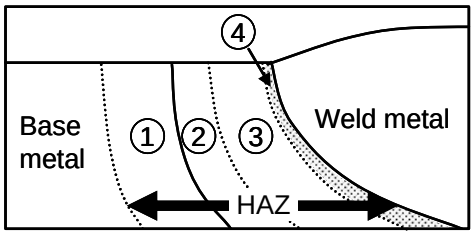

Fig. 3 Schematic diagram of HAZ microstructure which is formed by a single-pass TIG weld.

grains were observed at the region near HAZ2 and coarse grains were observed near region HAZ4 as this region was heated to just below $T_{\gamma\delta}$ (the temperature at which δ phase began to form)

HAZ4 ($T_{\gamma\delta}$<T< T_m) — Fresh martensite and δ-ferrite was formed during welding in this region as this is located next to the fusion line.

Fig. 4 shows the schematic diagram of the multi-pass TIG welding process and the thermal history of a weldment, and Fig 5 shows the magnified microstructure of the HAZ which was formed by the multi-pass weld and tested in this study. This microstructure can be interpreted on the basis of the highest temperature (T_{max}) achieved during welding as follows:

Region 1 (T_T<T_{max}<Ac_1) — This region was over-tempered several times during welding. The microstructure is the same as HAZ1.

Region 2 (Ac_1<T_{max}<Ac_3) — The microstructure of this region is the same as HAZ2 as it was once heated between Ac_1 and Ac_3, but also over-tempered several times by subsequent passes during welding.

Region 3 (Ac_3<T_{max}<$T_{\gamma\delta}$) — HAZ3 would correspond to this region, but no larger grains were observed probably because this region was also heated between Ac_1 and Ac_3 and over-tempered a few times.

Region 4 ($T_{\gamma\delta}$<T_{max}<T_m) — This region must form martensite and δ-ferrite during welding, as this is located next to the fusion line. δ-ferrite was not obvious, and the microstructure was similar to that of region 3. This is probably because this region was also heated over Ac_3 or Ac_1 once or twice, and over tempered several times by the multi-pass welding.

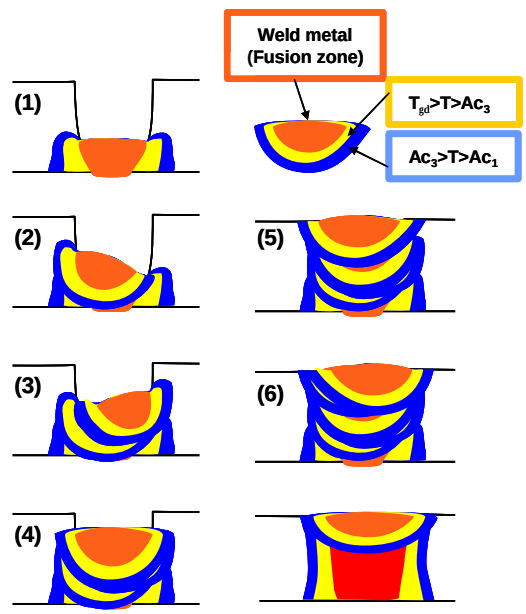

Fig. 4 Schematic diagram of the multi-pass TIG welding process and the thermal history of weldment

The microhardness profiles across the weld joint are shown in Fig. 6. Figure 6 (a) shows that minimum hardness was obtained for both unirradiated and irradiated specimens in the "over-tempered region," the region just next to the transformation line in region 1, which is denoted as A in Fig. 5. On the other hand, as shown in Fig. 6 (b), both minimum ΔHv and minimum hardening ratio were obtained at the "fine-grain region," the region which is located at about 1 mm from the transformation line in region 2, denoted as B in Fig. 5. The same hardness profile changes were also obtained in ion-irradiated TIG weldments [3].

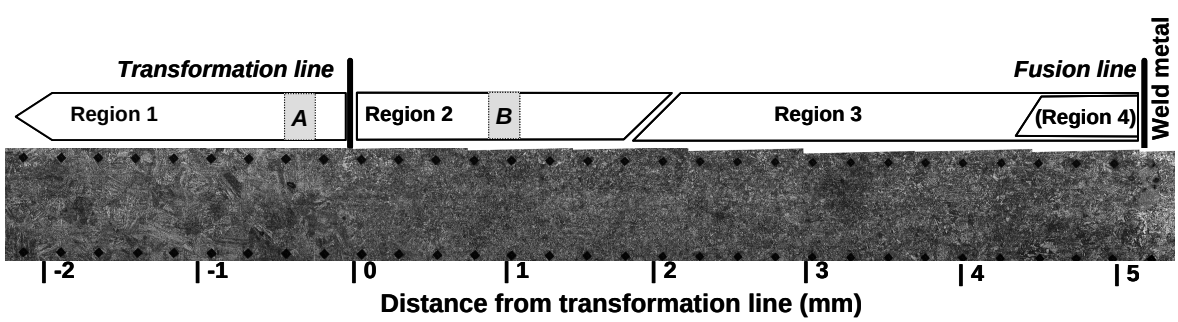

Fig. 5 Magnified image of HAZ and the definitions of the regions.

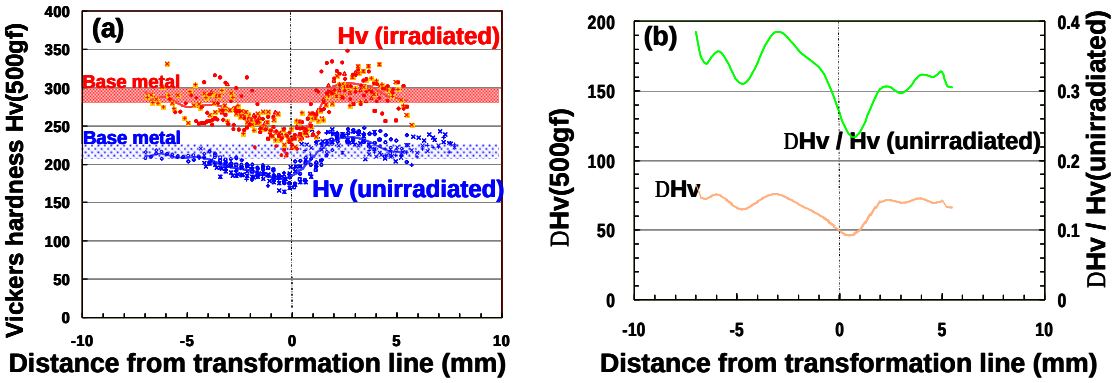

Fig. 6 The profile of (a) hardness and (b) hardness increase and the ratio of increase over irradiated and unirradiated weldments .

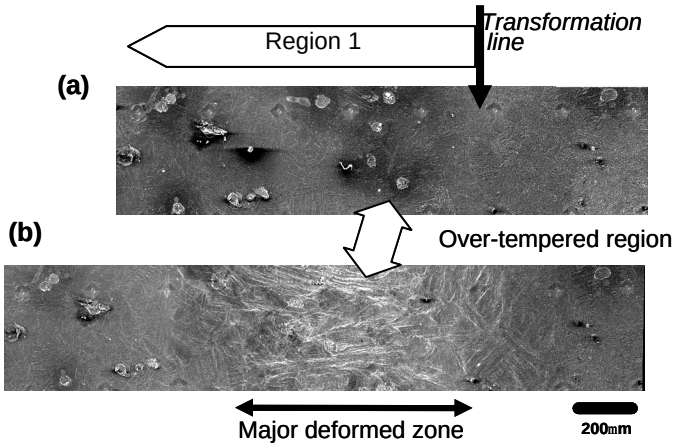

Fig. 7 Microstructure of (a) as-hardness-tested and (b) deformed weld joint tensile specimens .

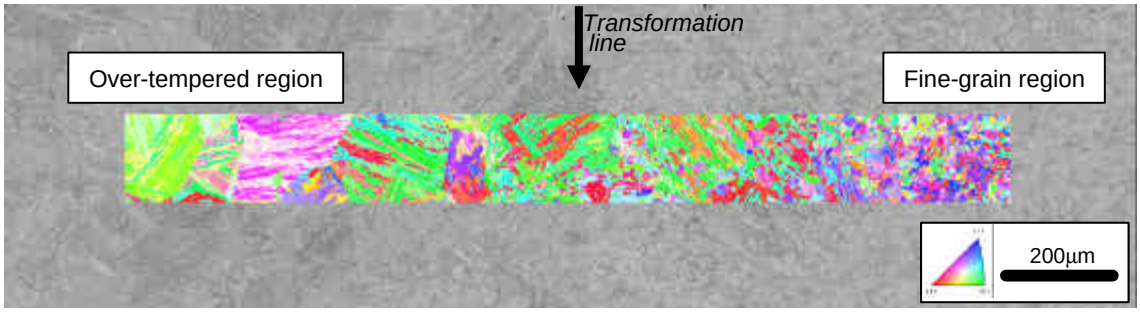

Fig.8 BSE images and OIM results plotted on the corresponding location of the weldment.

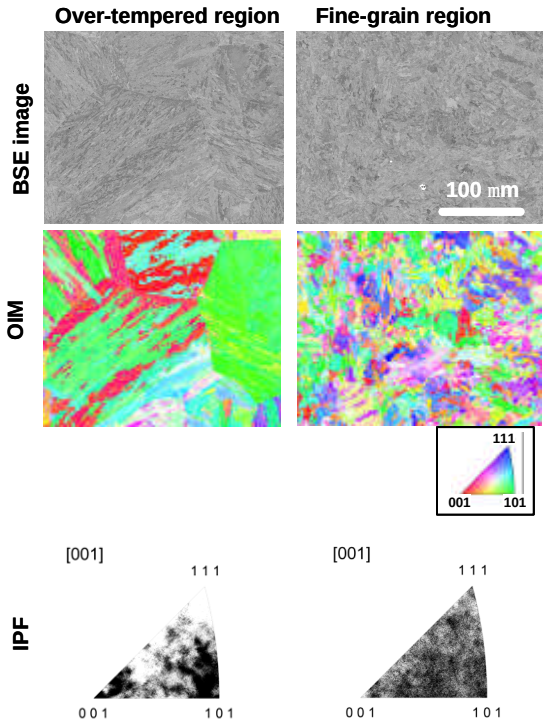

Fig. 9 BSE images with OIM and IPF results on over-tempered region and fine-grain region.

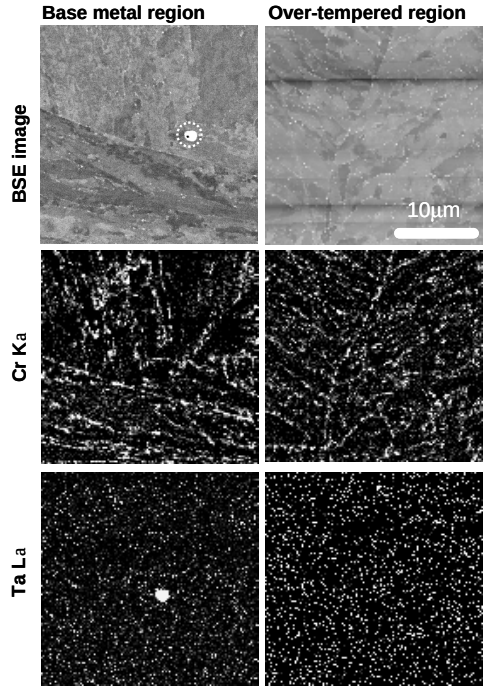

Fig. 10 BSE images and XEDS mapping results on base metal region and over-tempered region. The white dashed circle indicates the BSE image of a Ta-rich precipitate.

A tensile test was performed using the hardness-tested and observed tensile specimen to confirm the region where the major deformation occurred by stopping the tensile test before fracture. The region was identified by the hardness indents near by. As shown in Fig. 7, the major deformation occurred in the over-tempered region.

These results clearly indicate that the tensile results obtained from the weld joint specimen represent the tensile property of the over-tempered region, and the tensile property of the fine-grain region, which exhibited the minimum hardening ratio, is better than the over-tempered region.

Mechanism of low irradiation hardening

Figure 8 shows the OIM results across the transformation line placed on the back-scattered electron (BSE) image. The results show that the grains become fine and isotropic in the fine-grain region. The magnified images of the mapping of each region and inversed pole figure (IPF) are shown in Fig. 9. A triple point of the grain structure is included in both cases, although they are nondistictive in the fine-gain region. The fine-grain region consisted of isotropically oriented grains in which the shapes are related to the former lath or packet structure. IPF also suggests that those fine grains have an isotropic orientation, while the results from the over-tempered region suggest an anisotropic tendency. These results indicate that there are more high-index grain boundaries in the fine-grain region than in the base-metal, as there is no distinctive difference in grain structure between the base-metal region and the over-tempered region.

XEDS mapping was performed to analyze Cr-rich and Ta-rich precipitate distributions on the base-metal region and the over-tempered region (Fig.10). The Cr K_α and Ta L_α peaks were selected for mapping. The

results showed that the distribution of Cr-rich precipitates was similar in each region. The results also indicated that there were no detectable small-sized Ta-rich precipitates. On the other hand, precipitates with bright contrast in the BSE image turned out to correspond to large-sized (>1nm) Ta-rich precipitates, mainly consisting of Ta, Ti and V. These images are dominant both in the over-tempered region and base metal region, but not in the fine-grain region.

From these results, the following hypothetical mechanisms of low hardening for each region were derived:

The fine-grain region — Fine grain structures act as neutral sinks, where induced point defects have high probability to be absorbed and re-combined.

The over-tempered region — No clear evidence was obtained to explain the mechanism of low hardening in this region. One possible explanation which could be indicated from Fe-C phase diagram is that the heating during welding increased the solute carbon concentration. It has been postulated that the local strain field around carbon atoms can act as re-combination sites for irradiation-induced point defects.

Active point defect absorption and re-combination in these regions may result in far less hardening compared to the base metal region.

Hashimoto et.al. performed transmission electron microscopy to analyze the microstructures of these regions of the irradiated weldments [4], and it turned out that no visible dislocation loops were observed in the over-tempered region and the fine-grain region. Small dislocation loops were the main microstructural features in F82H irradiated up to 5 dpa at 573K. This result indicates that more active point defect absorption and re-combination took place in those regions, and this conforms to the hypothetical mechanisms proposed above.

SUMMARY AND CONCLUSIONS

An irradiated TIG weld joint of F82H IEA, which showed far less hardening than the base metal in previous post-irradiation tensile tests, was investigated by taking a hardness profile across the irradiated weld joint to locate the region that was involved with this low hardening. The following summarizes the observations and conclusions:

1. The hardness profile and the metallography indicated that the weakest part of the HAZ is in the over-tempered zone located in the region of the HAZ that was heated to just below the Ac_1, the temperature at which austenite begins to form on heating.
2. A tensile test halted before fracture revealed that the plastic deformation occurred at the lowest hardness region.
3. There is a low-hardening region in the fine-grain region that was heated between Ac_1 and Ac_3 during welding.
4. SEM observations and OIM analyses revealed that the fine-grain region consisted of isotropically oriented fine prior austenite grains.
5. The hypothetical mechanisms proposed for these low hardening regions is that those microstructures involve a high concentration neutral sinks for point defect recombination.

ACKNOWLEDGEMENT

The authors would like to thank E.A. Kenik for helping with the SEM analysis at SHaRE Collaboration Research Center at Oak Ridge National Laboratory. This research was sponsored by the Japan Atomic Energy Research Institute and the Office of Fusion Energy Sciences, US Department of Energy under contract DE-AC05-96OR22464 with UT-Battelle.

REFERENCE

[1] K. Shiba, R.L. Klueh, Y. Miwa, N. Igawa, and J.P. Robertson, Fusion materials semiannual progress report, DOE/ER-0313/28 (2000) 131
[2] R.L. Klueh and D.R. Harries, “High-Chromium Ferritic and Martensitic Steels for Nuclear Applications” ASTM, PA USA (2001), p72
[3] M. Ando, T. Sawai, E. Wakai, JAERI-Research (2002), to be published
[4] N. Hashimoto, M. Ando, H. Tanigawa, T. Sawai, K. Shiba, R.L. Klueh, to be published in this report.